Desalination 378 (2016) 92–99

Contents lists available at ScienceDirect

Desalination

journal homepage: www.elsevier.com/locate/desal

Exergetic efficiency of NF, RO and EDR desalination plants

Bilal Ahmed Qureshi [a], Syed M. Zubair [b,*]

[a] Center of Excellence for Scientific Research Collaboration With MIT, KFUPM Box # 1276, Saudi Arabia
[b] Mechanical Engineering Department, KFUPM Box # 1474, King Fahd University of Petroleum & Minerals, Dhahran 31261, Saudi Arabia

HIGHLIGHTS

- Exergetic analysis of a commercial-scale brackish water desalination plant is investigated.
- The plant contains nanofiltration, reverse osmosis and electrodialysis reversal units subject to the same source water.
- The correct definition of exergetic efficiency for such systems was discussed.
- It is shown that the calculated second-law efficiencies are very low.
- It is demonstrated that the highest efficiency occurred through use of a pressure exchanger.
- The pressure retarded osmosis option investigated had efficiencies approximately equal to the hydro-turbine.

ARTICLE INFO

Article history:
Received 23 June 2015
Received in revised form 23 September 2015
Accepted 28 September 2015
Available online 22 October 2015

Keywords:
Exergetic efficiency
Energy recovery device
Electrodialysis
Reverse osmosis
Pressure retarded osmosis

ABSTRACT

Exergetic analysis of a 2250 gpm brackish water desalination plant in California was performed using its operational data. The plant contains nanofiltration, reverse osmosis and electrodialysis reversal units subject to the same source water. The correct definition of exergetic efficiency for such systems was discussed. The effect of feed salinity was also used for further illustrating the difference in the second-law efficiency definitions. The preferred definition can be used to determine the specific energy consumption and makes thermodynamic sense. The nanofiltration, reverse osmosis and electrodialysis reversal units had efficiencies of 0.087%, 0.066% and 0.078%, respectively, which are very low. Various energy recovery devices including a pressure retarded osmosis unit (having infinite area) were applied to the system to see relative increase in second-law efficiency. For the preferred definition, it was seen that the nanofiltration unit had the best efficiency. In terms of alternative designs using energy recovery devices, the pressure retarded osmosis option had efficiencies approximately equal to the hydro-turbine while the highest efficiency occurred through the use of a pressure exchanger at the plant inlet salinity. Therefore, it does not seem to be a practical energy recovery method for the investigated desalination systems.

1. Introduction

Approximately 20% of the world's population lacks drinking water. About 25% may be living in water scarce areas by 2020 [1]. With the current world population above 7 billion and expected to reach 9 billion before 2050 [2], the need for potable water is expected to rise significantly. Desalination has been providing drinking water for decades and is used in 150 countries worldwide [3]. Desalination technologies include multi-stage flash distillation (MSF), nanofiltration (NF), reverse osmosis (RO), electrodialysis (EDR), multiple-effect distillation (MED) and vapor compression (VC). From these, reverse osmosis, which is a commercialized membrane-based process [4], represents 60% of total installed capacity [5]. For membrane-based technologies, the energy requirement of these systems can be lowered by combining it with other systems [6–12], producing enhanced membranes [13–15], using more efficient pumps and/or incorporating new or improved energy recovery methods [16–19]. Commercialized energy recovery devices include the Pelton turbine, turbocharger and pressure exchanger wherein the Pelton turbine is probably used the most [20].

Both the first-law (energy) as well as second-law basis (exergy) can be used to evaluate desalination plants with existing or new energy recovery devices. First law analysis focuses on the quantity of energy spent. In desalination systems, the specific energy consumption (SEC), which is the power consumed per cubic meter of fresh water produced, may be taken as a quantitative measure of the energy consumed. Second law analysis focuses on the quality aspect of the energy consumed (i.e. exergy). The reversible work that be done by a system is characterized by its exergy with respect to a dead state or the environment. Exergy analysis not only highlights component irreversibilities

* Corresponding author.
E-mail address: smzubair@kfupm.edu.sa (S.M. Zubair).

http://dx.doi.org/10.1016/j.desal.2015.09.027

but also assesses the efficiency of the overall system. Fitzsimons et al. [21] reviewed six exergy model approaches with focus on the chemical exergy term. They showed that the choice of exergy model can have a significant effect on the results, which coincides with the conclusions of Sharqawy et al. [16,22]. Also, they mentioned some concerns regarding three of the models such as that used by Cerci [23,24]. Second-law (exergetic) efficiency is found in the literature to be often defined in two ways. The first method says that it is the ratio of total exergy leaving divided by total exergy entering the system. The second is defined as the ratio of the product to fuel exergies [25,26]. For example, Kahraman et al. [27] and Sharqawy et al. [16] applied the first definition while Demirel [28] and Mistry et al. [29] used the second method. Section 2.2 focuses on resolving this issue. Other definitions such as the rational efficiency have been mentioned in the context of thermal plants by Kotas [30] and compared to the above and other efficiency definitions by Cornelissen [31] and Fitzsimons [32].

Many researchers have performed exergy analyses of membrane-based desalination plants and identified the sources of irreversibility in them. For example, Kahraman et al. [27] performed exergy analysis of a two-stage RO, NF and EDR desalination plant located in California with brackish water feed and no ERD. The second-law efficiencies were found to be 8%, 9.7% and 6.3% with the largest amount of exergy destruction occurring in the RO modules (36.2%–48.6%) and pumps (23.6%–54.1%). Second-law analysis of a two-stage RO desalination plant with brackish water feed was performed by Aljundi [33]. With no energy recovery device, the exergetic efficiency was found to be 4.1%. Exergy destruction in the four throttle valves was about 57% and approximately 21% in the RO modules. A two-stage industrial RO unit was analyzed by Gasmi et al. [34] and it was found that approximately 55% of the exergy destruction came from the pumps while the RO modules constituted 37%. Using seawater as feed, Blanco-Marigorta et al. [35] performed second-law analysis of a two-stage RO desalination plant. The exergetic efficiencies were determined to be 26.8%, 28.4% and 32.8% when the ERD used was a pressure exchanger, a Pelton turbine and a Dual Work Exchange Energy Recovery system, respectively. The RO modules and the high-pressure pump were reported as the main sources of irreversibility. Liu et al. [36] did exergy analysis of a dual-stage nanofiltration seawater desalination unit. The exergetic efficiency was found for three scenarios: i) no ERD (38.88%), ii) with ERD (51.82%), and iii) with ERD and blending (46.11%). The membrane modules and throttle valves were locations of the largest exergy destruction. Exergy analyses of single-stage systems indicated similar results [16–18,24,37,38]. Also, it should be noted that these diverse exergetic efficiency values are due to differences in some or all of the following factors: feedwater salinity, flow rate, pump efficiency, choice of energy recovery device, efficiency definition and exergy destruction in the throttle valves.

In this paper, the modeling of the energy recovery devices is done in Section 2 along with selection of the appropriate definition of the second-law efficiency for membrane-based desalination plants. Then its link to the specific energy consumption is established. In Section 3, the second-law efficiency and specific energy consumption for a case study dealing with (two-stage) reverse osmosis, (two-stage) nanofiltration and electrodialysis desalination plants are determined. Then various energy recovery devices are applied to the original systems including pressure retarded osmosis for comparative analysis.

2. Modeling

The assumptions made are as follows:

- In the ERDs, pressure drops in the lines are not considered.
- Fluid in the ERD is considered at a constant environmental temperature of 15 °C.
- Seawater properties are determined from the correlations given by Sharqawy et al. [39].
- The efficiency of the turbocharger is taken as 70% [20] while it is assumed to be 85% for the turbines [20,40].
- Leakage is assumed to be zero in the pressure exchanger while its efficiency is taken as 96% [41] unless otherwise indicated.
- The properties of the PRO intake are the same as that at the main feed pump i.e. $T_0 = 15\,^{\circ}C, P_0 = 101.325\ \ kPa, S_0 = 0.9\ \ g/kg$(dead state).
- Effect of reverse salt diffusion and concentration polarization are ignored in the PRO.
- For the PRO modules, an infinite area (unit effectiveness) is assumed.

2.1. First-law analysis

For the purpose of understanding the two definitions of the exergetic efficiency discussed in Section 2.2, modeling of the above systems involve applying mass and solution balances (Eqs. (1) and (2), respectively, below) on the RO and PRO module as well as between any two consecutive states.

$$\sum_{in} \dot{m} = \sum_{out} \dot{m} \tag{1}$$

$$\sum_{in} \dot{m}S = \sum_{out} \dot{m}S \tag{2}$$

The electrical input to the pumps is related to the ideal pumping power by its isentropic efficiency while the turbine power produced is found by multiplying its isentropic efficiency with the ideal turbine power.

$$\dot{W}_{pp} = \frac{\dot{W}_{is,pp}}{\eta_{is,pp}} \tag{3a}$$

$$\dot{W}_t = \eta_{is,t} \dot{W}_{is,t} \tag{3b}$$

As in the turbine, power extracted from the turbocharger is found by using its efficiency in Eq. (3b).

The efficiency of the pressure exchanger is defined as [42]:

$$\eta_{px} = \frac{\sum_{out} \left(\dot{V}P\right)}{\sum_{in} \left(\dot{V}P\right)} = \frac{\dot{V}_{B,o}P_{B,o} + \dot{V}_{f,o}P_{f,o}}{\dot{V}_{B,i}P_{B,i} + \dot{V}_{f,i}P_{f,i}} \tag{4}$$

In the PRO unit working as an ERD, the mixing (or mass) ratio (MR) is defined as the ratio of the mass flow rates of the draw solution to the incoming feed water [43].

$$MR = \frac{\dot{m}_{d,i}}{\dot{m}_{f,i}} \tag{5}$$

For the PRO unit, the maximum recovery ratio (see Eq. (6) below) is used at the chosen mass ratio. The model developed by Sharqawy et al. [43] is used to find this maximum for an optimized hydraulic pressure difference calculated using a program written in EES [44].

$$R_{PRO} = \frac{\dot{m}_p}{\dot{m}_{f,i}} \tag{6}$$

Lastly, the specific energy consumption of the desalination unit is calculated by dividing the net power requirement by the permeate flow rate.

$$SEC = \frac{\dot{W}_{in}}{3600\dot{V}_p} \tag{7}$$

This concludes mentioning of the key equations required for system modeling.

2.2. Second-law analysis

Studies, such as [16,27,33–35,37], have shown the common sources of irreversibility in membrane-based desalination systems. Therefore, this study focuses on correctly determining the second-law efficiency. The literature contains two definitions for the second-law efficiency [25]. The first definition follows the exergy balance shown in Eq. (8a). It says that the exergy destroyed is the difference between all the incoming and outgoing exergies:

$$\sum_{in}\dot{X}-\sum_{out}\dot{X}=\dot{X}_D \tag{8a}$$

In this case, second-law efficiency is defined as

$$\eta_{II,Rg0}=\frac{\sum_{out}\dot{X}}{\sum_{in}\dot{X}}x100=\left(1-\frac{\dot{X}_D}{\sum_{in}\dot{X}}\right)x100 \tag{8b}$$

The sum of all the incoming exergies consists of net power/electrical input as well as the streams. The difference between the sum of the outlet and inlet stream exergies is called the least work of separation (Eq. 8(c) below).

$$\dot{W}_l=\sum_{out}\dot{X}-\sum_{in}\dot{X} \tag{8c}$$

This is the reversible work needed to produce the required permeate for a finite recovery ratio (i.e. R > 0) [29]. When the input streams are taken as the dead state, the second-law efficiency is given as:

$$\eta_{II,Rg0}=\frac{\dot{W}_l}{\dot{W}_{in}}x100 \tag{8d}$$

The second definition follows the exergy balance shown in Eq. (9a). It says that the sum of exergy destroyed and lost is equal to the difference between the sum of the fuel and product exergies:

$$\sum_{fuel}\dot{X}-\sum_{products}\dot{X}=\dot{X}_D+\dot{X}_L \tag{9a}$$

In this case, exergetic efficiency is defined as

$$\eta_{II,R0}=\frac{\sum_{products}\dot{X}}{\sum_{fuel}\dot{X}}x100=\left(1-\frac{\dot{X}_D+\dot{X}_L}{\sum_{fuel}\dot{X}}\right)x100 \tag{9b}$$

The least work of separation related to this method is described by Mistry et al. [29] to be the minimum value of $\dot{W}_l$. It is determined by calculating the difference between the sum of the product and fuel stream exergies:

$$\dot{W}_{l,\,min}=\sum_{products}\dot{X}-\sum_{fuel}\dot{X} \tag{9c}$$

This is the reversible work needed to produce the required permeate for an infinitesimal recovery ratio (i.e. R = 0). Now, when the input streams are taken as the dead state, their sum becomes equal to the sum of the fuel exergies [29]. The second-law efficiency is then given by:

$$\eta_{II,R0}=\frac{\dot{W}_{l,\,min}}{\dot{W}_{in}}x100 \tag{9d}$$

Comparing the efficiency definitions shows that the numerator constitutes the only difference between them. With respect to work of least separation, the difference in these two definitions occurs due to differing ways in considering the disposal of the brine stream. In Eq. (8c), the exergy of the brine stream is considered as part of the $\sum_{out}\dot{X}$ term because it is an exiting stream. On the other hand, it is not used in Eq. (9c) in this way because it is not a product (nor a fuel). Instead, it is taken as exergy lost by the system. Mistry et al. [29] argued that the latter definition was correct because the minimum least work of separation represented the actual exergetic value of the product water. The current authors would further reason that because the brine exergy is lost, it should not help to increase the exergetic efficiency. On close examination, it is seen from Eq. (8d) that this is precisely what happens but not in Eq. (9d) since it correctly considers the brine stream as exergy lost. Therefore, the latter method of defining the exergetic efficiency is considered as the correct one. Another point to be noted is that there is a simple way to unite the two exergetic efficiency definitions. This is done by taking into account the process of brine disposal into the source (such as part of the same river at another location) by extending the control volume. Therefore, this exiting stream would now have zero exergy and, thus, not affect the value of the numerator of Eq. (8d) resulting in the same exergetic efficiency as Eq. (9d). This leads to answering a basic question and that is the extent of the control volume, which constitutes the system. This also shows that, if the control volume is properly defined, the first definition of the exergetic efficiency simply turns out to be a special case of the second definition.

Finally, it is important that the exergetic efficiency defined should be meaningful from a thermodynamic as well as economic perspective [25]. Now, since the product of the desalination systems is the permeate exergy and the sum of input exergies is the net pumping/electrical power (input stream is at dead state), a comparison of Eqs. (9c), (9d) and (7) show that the exergetic efficiency and SEC are inversely proportional to each other. They are separated by a simple product of the permeate specific exergy and density combined with a conversion factor as shown below:

$$\eta_{II,R0}=\frac{\rho_p x_p}{36(SEC)} \tag{10}$$

where ρ_p and x_p are the density and specific exergy, respectively, of the permeate.

3. Case study: NF, RO and EDR plant

In this section, an exergy analysis is performed for desalination plants previously presented by Kahraman et al. [27]. The plant contains full scale NF, RO and EDR units being fed from the same source water. Figs. 1(a)–(c) show schematics of these units that are located in California, USA. It has a potable water production capacity of around 2250 gal per minute having a salinity of 0.37 g/kg (370 ppm). The source water is brackish in nature with a salinity of 0.9 g/kg, 101.325 kPa pressure and 15 °C temperature.

In the RO unit, the first pump raises the pressure of the brackish water to 667 kPa while the second pump boosts the pressure to 1011 kPa. The saline water then enters the two-stage RO unit that results in a brine of 3.41 g/kg and product water of 0.064 g/kg (64 ppm). This is blended with the source water in a mixing chamber resulting in the target salinity of 0.37 g/kg. Finally, this stream goes through a degasifier to remove dissolved gases and is ready for use. The average power input of the plant for June, 2000 was determined to be 76.95 kW. The NF unit operates similarly with the difference that the second pump boosts the pressure to 922 kPa. Also, the dual-stage NF membranes provide brine and permeate with salinity of 3.21 g/kg and 0.124 g/kg, respectively. The average electrical power input to the plant was calculated to be 57.84 kW. The EDR unit differs from the other two units in the sense that it does not have a booster pump and

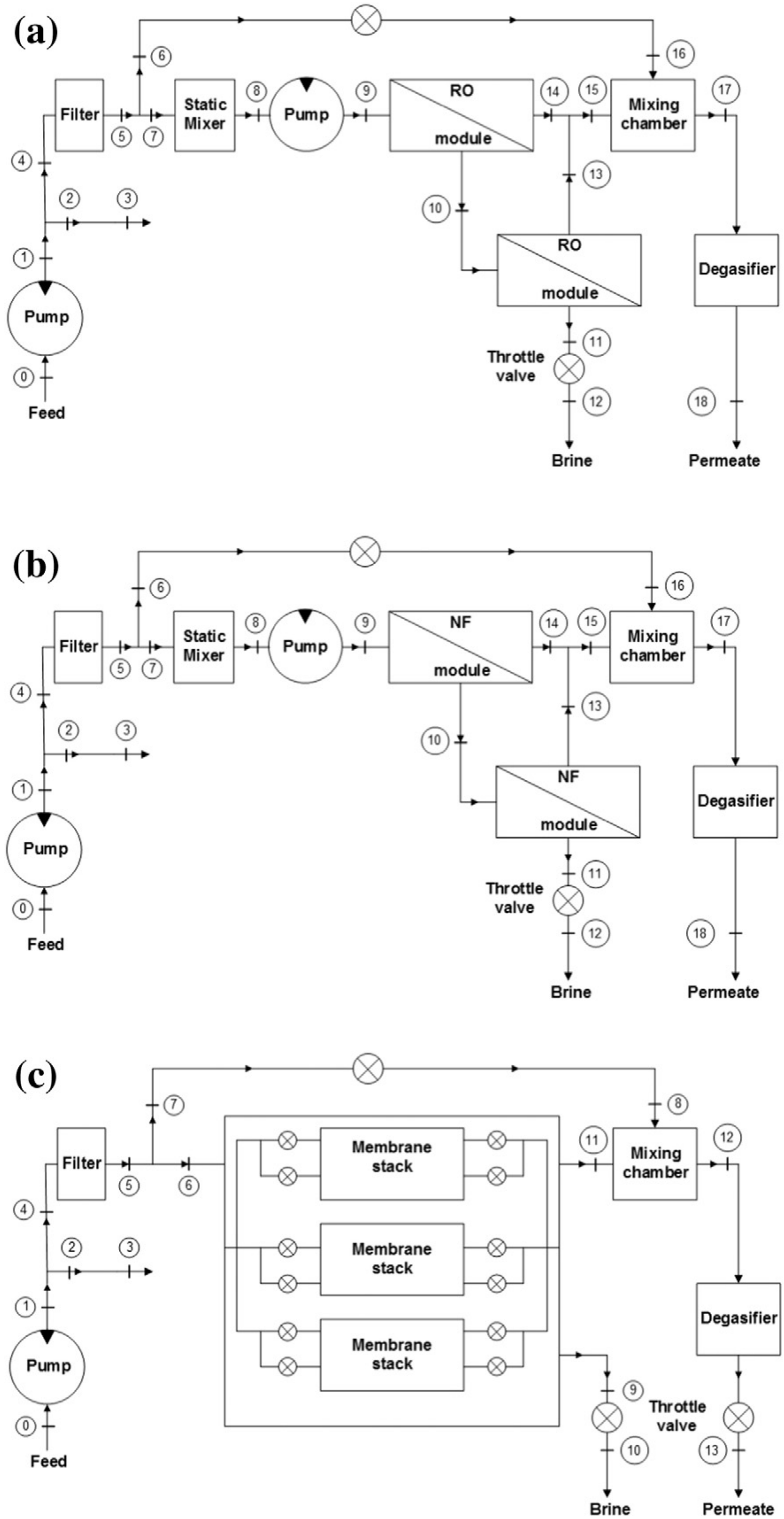

Fig. 1. (a). RO unit schematic of the desalination plant. (b). NF unit schematic of the desalination plant. (c). EDR unit schematic of the desalination plant.

neither is there blending in the mixing chamber. Also, the brine salinity at the exit of the membrane stacks is 4.89 g/kg while the product water is at the target salinity. The average electrical power consumption of the plant was found to be 57.37 kW.

Tables 1–3 contain data for all the states of the RO, NF and EDR plants, respectively, representing averaged monthly data for June, 2000. These tables also contain specific exergy values determined by Kahraman et al. [27] as well as those determined by accurate sea

Table 1
Properties and exergies at all states of the RO plant.

State	P (kPa)	S (g/kg)	$\dot{m}$ (kg/s)	x^a (kJ/kg)	x^b (kJ/kg)	Error (%)	$\dot{X}^b$ (kW)
0	101.325	0.9	59.010	0	0	0	0
1	667	0.9	59.010	0.5648	0.5659	0.1933	33.393
2	667	0.9	1.6420	0.5648	0.5659	0.1933	0.929
3	101.325	0.9	1.6420	0	0	0	0
4	667	0.9	57.368	0.5648	0.5659	0.1933	32.464
5	638	0.9	57.368	0.5359	0.5369	0.183	30.800
6	638	0.9	17.333	0.5359	0.5369	0.183	9.306
7	638	0.9	40.035	0.5359	0.5369	0.183	21.494
8	623	0.9	40.035	0.5209	0.5219	0.1871	20.893
9	1011	0.9	40.035	0.9083	0.91	0.1897	36.433
10	804	1.4018	25.018	0.5385	0.7036	23.47	17.604
11	701	3.4104	10.002	−0.1581	0.6225	125.4	6.226
12	205	3.4104	10.002	−0.7554	0.02377	3278	0.238
13	205	0.064	15.017	0.4103	0.1065	285.3	1.599
14	205	0.064	15.017	0.4103	0.1065	285.3	1.599
15	205	0.064	30.033	0.4103	0.1065	285.3	3.198
16	205	0.9	17.333	0.1035	0.1037	0.2074	1.798
17	205	0.37	47.367	0.2889	0.1048	175.6	4.966
18	101.325	0.37	47.367	0.1853	0.001086	16,967	0.051

[a] Kahraman et al. [24].
[b] Present work.

water properties provided by Sharqawy et al. [39]. The large deviations are visible whenever the chemical exergy calculation is involved due to variation of salinity from the dead state. The largest deviation is found for the permeate in all the plants. Besides large deviations, sometimes negative values for the specific exergy for the model of Kahraman et al. [27] are also seen. This is due to the fact that, in their model, seawater is considered as an ideal mixture (pure water plus Sodium Chloride) because of which the flow exergy has negative values at salinities higher than the dead state. This is because the chemical exergy portion was not appropriately accounted for in this model [22].

It is again emphasized that since the common sources of exergy destruction in membrane-based desalination systems have been pointed out in previous studies, we will currently focus on the second-law efficiency. The minimum value for the least work of separation is equal to the exergy of the permeate (see Section 2.2). The last entry in Tables 1–3 shows that the RO plant has the highest value simply because the mass flow rate is higher in it. Contrary to this, the RO plant also has the highest power input requirement, which is (on average) 33.5% greater than the other two units. This large difference in power input outweighs any effect of higher permeate exergy on second-law efficiency. Using Eq. (9d), the exergetic efficiency of the nanofiltration, reverse osmosis and electrodialysis reversal units are found to be 0.087%, 0.066% and 0.078%, respectively, which are very low.

Table 2
Properties and exergies at all states of the NF plant.

State	P (kPa)	S (g/kg)	$\dot{m}$ (kg/s)	x^a (kJ/kg)	x^b (kJ/kg)	Error (%)	$\dot{X}^b$ (kW)
0	101.325	0.900	58.210	0	0	0	0
1	667	0.900	58.210	0.5648	0.5659	0.1933	32.941
2	667	0.900	1.200	0.5648	0.5659	0.1933	0.679
3	101.325	0.900	1.200	0	0	0	0
4	667	0.900	57.010	0.5648	0.5659	0.1933	32.262
5	638	0.900	57.010	0.5359	0.5369	0.183	30.608
6	638	0.900	14.702	0.5359	0.5369	0.183	7.893
7	638	0.900	42.308	0.5359	0.5369	0.183	22.714
8	623	0.900	42.308	0.5209	0.5219	0.1871	22.080
9	922	0.900	42.308	0.8195	0.821	0.1818	34.735
10	708	1.364	26.472	0.4546	0.6075	25.17	16.082
11	550	3.212	10.633	−0.2526	0.4682	153.9	4.979
12	101.325	3.212	10.633	−0.6996	0.02019	3566	0.215
13	198	0.124	15.838	0.3776	0.0991	281	1.570
14	198	0.124	15.838	0.3776	0.0991	281	1.570
15	198	0.124	31.675	0.3776	0.0991	281	3.139
16	198	0.900	14.702	0.0965	0.09671	0.2196	1.422
17	198	0.370	46.377	0.1853	0.09784	89.39	4.537
18	101.325	0.370	46.377	0.1853	0.001086	16,967	0.050

[a] Kahraman et al. [24].
[b] Present work.

Table 3
Properties and exergies at all states of the EDR plant.

State	P (kPa)	S (g/kg)	$\dot{m}$ (kg/s)	x^a (kJ/kg)	x^b (kJ/kg)	Error (%)	$\dot{X}^b$ (kW)
0	101.325	0.900	50.075	0	0	0	0
1	667	0.900	50.075	0.5648	0.5659	0.1933	28.3371
2	667	0.900	3.030	0.5648	0.5659	0.1933	1.7147
3	101.325	0.900	3.030	0	0	0	0
4	667	0.900	47.045	0.5648	0.5659	0.1933	26.6225
5	638	0.900	47.045	0.5359	0.5369	0.183	25.2576
6	638	0.900	47.045	0.5359	0.5369	0.183	25.2576
7	638	0.900	0.000	0.5359	0.5369	0.183	0
8	157	0.900	0.000	0.0556	0.0557	0.1733	0
9	157	4.890	5.517	−1.102	0.1148	1059	0.6336
10	101.3	4.890	5.517	−1.157	0.05932	2051	0.3273
11	157	0.370	41.528	0.241	0.05681	324.3	2.3590
12	157	0.370	41.528	0.241	0.05681	324.3	2.3590
13	101.325	0.370	41.528	0.1853	0.001086	16,967	0.0451

[a] Kahraman et al. [24].
[b] Present work.

On close inspection, it is understood that these very low values are not completely unexpected. To understand this better, let us take the work of Sharqawy et al. [16], wherein a single-stage RO plant with brackish water feed of 1.55 g/kg was analyzed based on the second-law. It should be noted that, while this system is not exactly the same as the RO unit under consideration, the fact that it is a brackish water plant which is assessed using the same accurate seawater properties [39] used in this work, would still provide an appropriate example. In [16], the first thing to note is that the use of the accurate seawater properties resulted in an exergetic efficiency that was 2.85 times lower than originally reported by Cerci [24]. This indicates that lower values of exergetic efficiency are expected in the current work compared to those calculated by Kahraman et al. [27]. The second thing to note is that the exergetic efficiency definition used is equal to Eq. (8d) while, in the current work, Eq. (9d) is used. Furthermore, the pump efficiency was assumed to be 100% while this is not the case in the current work. This is important to consider since it would significantly increase the quantity in the denominator of the exergetic efficiency formula. To determine the exergetic efficiency of the plant in [16] using Eq. (9d), we see from the last entry of Table 1 in [16], that the exergy of the permeate is 0.5853 kW. From Table 2 of [16], it is found that the total pumping power is 165.74 kW for a pumping efficiency of 100%. Kahraman *et al.* [27] determined that the pumping efficiency of the RO unit was 63.5%. If this same efficiency is used, then the power input for the plant in [16] would increase to 261 kW resulting in a second-law efficiency of 0.224%. This shows that, as long as the basis for the second-law efficiency is the same, the values do not differ greatly.

3.1. Alternative designs using energy recovery devices

Now, it is clear that the energy input requirement is much higher than the exergy of the product and that the very low second-law efficiencies are due to large exergy destruction in the components such as the membranes and the throttle valves. We will currently focus on the latter component, as reducing exergy destruction in the membrane would require altering its characteristics. Therefore, we can replace the throttle valve for the brine flow with different energy recovery devices. The common ERDs include the turbocharger, hydro-turbine and pressure exchanger while, in the current work, a pressure retarded osmosis (PRO) [45,46] unit with hydro-turbines will also be considered to determine its viability due to it being introduced as an energy recovery method by Sharqawy et al. [16].

Figs. 2(a)–(d) are schematics of the above-mentioned ERDs connected to the two-stage RO unit discussed previously (see Fig. 1(a)). The alternative designs for the NF and EDR units are similar. With the use of a throttling valve representing the base case for each unit, the purpose is not only to see the increase in efficiency due to using the common ERDs but also to evaluate PRO as an energy recovery method based on Eq. (9d). For PRO, the mixing ratio was varied from 1 to 10 [47]. It should be noted that, in the PRO units, the hydraulic pressure difference between the draw and the feed, ΔP, was not assumed to be equal to $\Delta\pi/2$ [48]; rather its optimized value was determined in each case. Also, the area was assumed to be infinite in the PRO options so as to establish an upper limit on their second-law efficiencies. Since Eq. (7) establishes the relation between exergetic efficiency and specific energy consumption, the SEC values in each case would also be of interest.

Table 4 provides a summary of second-law efficiencies and SEC values for the scenarios discussed above. With respect to the chosen definition of exergetic efficiency, it is seen that the turbo-charger has the lowest performance followed by the hydro-turbine and the pressure exchanger. It is seen that when the PRO unit is connected to each type of desalination plant, the system exhibits second-law efficiencies (and SEC values) approximately equal to the hydro-turbine. It is noted that the turbine is a simpler option and the effect of finite area and concentration polarization would further reduce the efficiency of the system using the PRO unit. The pressure exchanger as an ERD provides the best efficiency for all cases. The highest second-law efficiency of 0.0968% was obtained when the pressure exchanger was used with the NF unit. The pressure exchanger was not evaluated using the EDR desalination unit because only a pressure of 157 kPa was available to the brine stream compared to 550 kPa and 701 kPa for the NF and RO units, respectively. In contrast to these results, when Eq. (8d) is used to determine exergetic efficiency, we see the following differences:

- Electrodialysis has the highest efficiency in all cases.
- For the PRO as an ERD, it has an efficiency less than when the turbocharger is used except for the EDR technology. In that case, it has an efficiency less than the original system.
- The SEC values do not correspond to the above-mentioned changes.

This shows that the choice of efficiency formula cannot only have a significant effect on the value itself but also on comparative analysis of different desalination technologies.

3.2. Exergetic efficiencies vs. feed salinity

Now, the feed salinity of the systems analyzed in the previous section was low. In order to further understand the difference in the two definitions of the exergetic efficiency discussed in Section 2.2, the effect of brackish water feed salinity up to 10 g/kg [4] is investigated. Since the NF unit showed the best efficiency according to the chosen definition, it is used for this purpose. The system was modified to remove states 2 and 3 as the flow was becoming negative at higher salinities. For the purpose of demonstration, the original pressure drops in

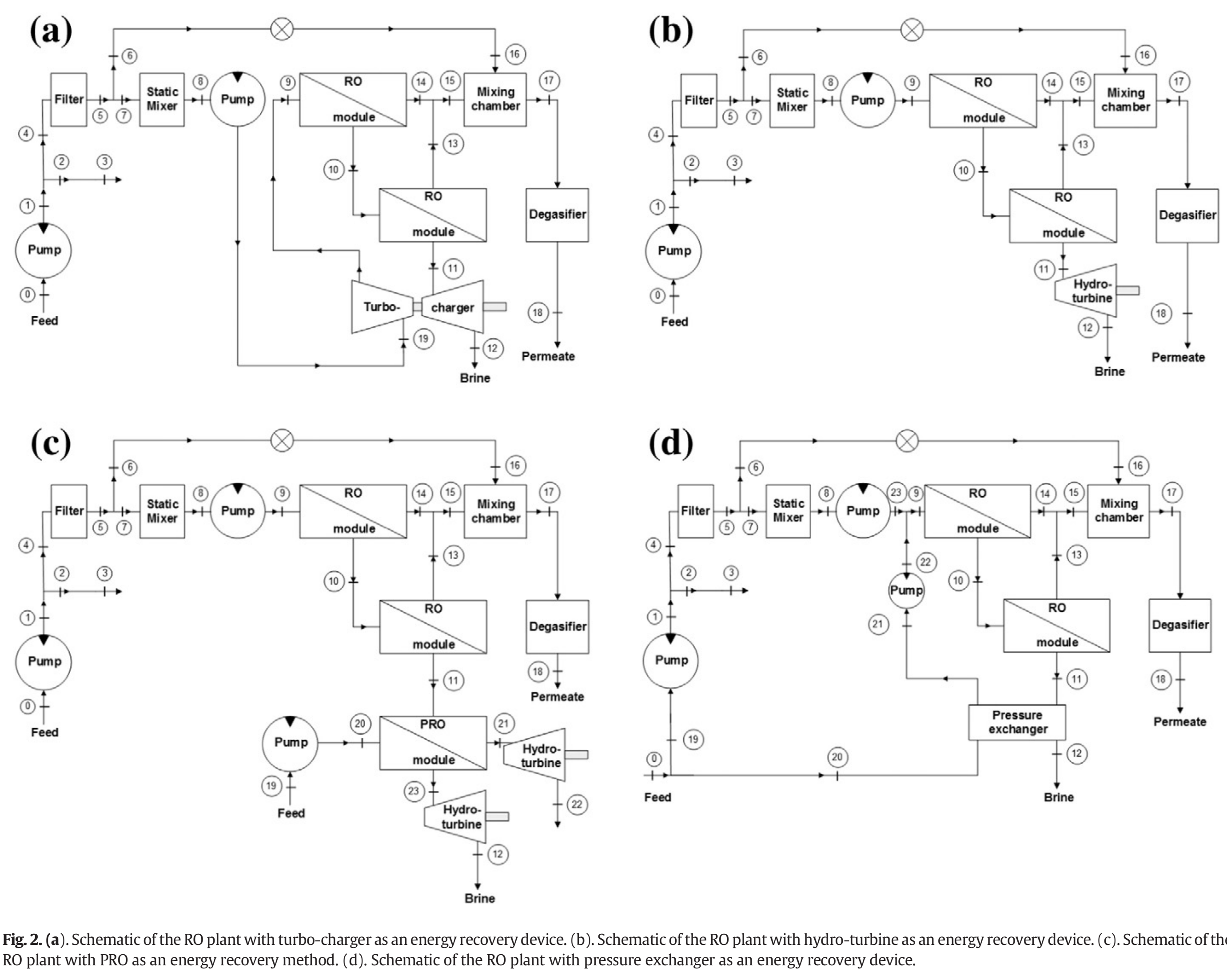

Fig. 2. (a). Schematic of the RO plant with turbo-charger as an energy recovery device. (b). Schematic of the RO plant with hydro-turbine as an energy recovery device. (c). Schematic of the RO plant with PRO as an energy recovery method. (d). Schematic of the RO plant with pressure exchanger as an energy recovery device.

Table 4
Summary of second-law efficiencies (%) and specific energy consumption (kWh/m^3) for all desalination unit configurations.

ERD	RO			NF			EDR		
	$\eta_{II,Rg0}$	$\eta_{II,R0}$	SEC	$\eta_{II,Rg0}$	$\eta_{II,R0}$	SEC	$\eta_{II,Rg0}$	$\eta_{II,R0}$	SEC
None	0.3758	0.0668	0.4509	0.4582	0.0871	0.3462	0.6491	0.0786	0.3834
Turbocharger	0.3974	0.0707	0.4263	0.4862	0.0924	0.3262	0.6515	0.0789	0.3820
PRO	0.3817	0.0715	0.4217	0.4681	0.0935	0.3223	0.6017	0.0790	0.3816
Hydro-turbine	0.4024	0.0716	0.4211	0.4926	0.0936	0.3219	0.652	0.0790	0.3817
Pressure exchanger	0.4249	0.0756	0.3988	0.5095	0.0968	0.3113	–	–	–

each of the NF modules were kept constant. This was 214 kPa for the first module and 158 kPa for the second. Also, the driving potential ($\Delta P - \Delta\pi$) for the second NF module was fixed at the original value of 422.3 kPa. This allowed for the hydraulic pressure at the inlet of the first NF module (state 9) to remain as a free variable and was determined according to these constraints as the feed salinity increased. The modified van't Hoff coefficient at 15 °C applicable for a salinity range of 0–35 g/kg was determined to be 70.703 kPa (compared to 73.07 kPa at 25 °C [43]). Details of the procedure can be found in Appendix A.1 of [43] and Appendix B of Banchik [19].

Fig. 3 shows the effect of feed (dead state) salinity on the exergetic efficiencies where the feed salinity of the original plant was taken as a starting point. The grayed area represents the typical feed salinity range for low-pressure nanofiltration membranes [4]. It is noted that, at salinities as low as in the original plant, the difference in the efficiencies is small but the difference increases non-linearly as the feed salinity increases. The absolute difference at salinities of 0.9, 5 and 10 g/kg are 0.33%, 12.16% and 26.8%, respectively. It should be noted that, at a feed salinity of 10 g/kg, the only reason the exergetic efficiency reaches ~37% (according to Eq. (8d)) is the fact that the salinity of the brine (state 12) increases to ~48 g/kg. Thus, the exergy of the brine becomes correspondingly large. This would mean that the more saline the wasted brine stream, the higher the efficiency. In view of the authors, this does not make thermodynamic sense. Hence, it is best to use Eq. (9d) for determining exergetic efficiency of the desalination systems investigated.

4. Concluding remarks

The exergetic efficiency of the plant is 0.087% for nanofiltration, 0.066% for reverse osmosis and 0.078% for electrodialysis reversal units using the same source water. The very low efficiency values show a large room for improvement such as the conversion of the electrical energy input into fluid power. The exergetic efficiency definition in these systems was discussed wherein the exergy of the products over the fuel exergy was used. This definition resulted in the possibility of determining the specific energy consumption from the exergetic efficiency. Well-known energy recovery devices as well as a pressure retarded osmosis unit (having infinite area) were applied to these systems to see the comparative change in exergetic efficiencies using both definitions as well as specific energy consumptions. For the preferred definition, the nanofiltration unit always displayed the best efficiency wherein the highest efficiency occurred with the pressure exchanger at the plant inlet salinity. The pressure retarded osmosis option studied had efficiencies approximately equal to the hydro-turbine. Therefore, considering the decrease in exergetic efficiency due to limitations of concentration polarization and finite area, it does not seem to be a viable energy recovery method for the desalination systems considered. Variation of both exergetic efficiencies with respect to feed salinity indicated that an efficiency that provides higher values simply due to a more saline (wasted) brine stream does not make thermodynamic sense. Thus, it is best to use the definition that uses the exergy of the permeate as a measure of system efficiency.

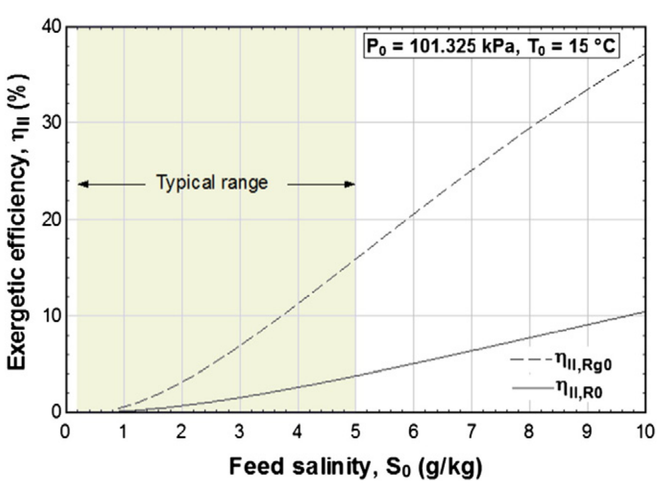

Fig. 3. Variation of the second-law efficiencies with respect to feed salinity for modified NF unit in Kahraman et al. [24].

Nomenclature

EDR	electrodialysis reversal
ERD	energy recovery device
$\dot{m}$	mass flow rate (kg/s)
P	pressure (kPa)
MR	mass or mixing ratio
NF	nanofiltration
R	recovery ratio
RO	reverse osmosis
S	salinity (g/kg)
SEC	specific energy consumption (kWh/m^3)
T	temperature (°C)
$\dot{V}$	volumetric flow rate (m^3/s)
x	specific exergy (kJ/kg)
$\dot{X}$	exergy (kW)
$\dot{W}$	power requirement (kW)

Greek symbols

ρ	density (kg/m^3)
η_{is}	isentropic efficiency (−)
η_{px}	pressure exchanger efficiency (-)
η_{II}	second-law (or exergetic) efficiency (%)
π	osmotic pressure (kPa)

Subscripts

B	brine
d	draw
D	destroyed
f	feed
i	entering
l	least
L	lost
min	minimum
o	exiting
p	permeate
pp	pump
px	pressure exchanger
R0	based on infinitesimal recovery ratio

Rg0 based on finite recovery ratio
t turbine

Acknowledgments

The authors acknowledge support from the King Fahd University of Petroleum and Minerals (KFUPM) through the Center for Clean Water and Clean Energy at MIT and KFUPM under Project Number R15-CW-11. Syed Zubair also acknowledges support from KFUPM through the project IN121042.

References

[1] National Geographic Magazine, Water: Our Thirsty World, 2010.

[2] U. Nations, World Population Prospects the 2012 Revision, New York, 2013 http://esa.un.org/wpp/Documentation/pdf/WPP2012_KEYFINDINGS.pdf.

[3] International Desalination Association, Desalination by the Numbers, 2014 http://idadesal.org/desalination-101/desalination-by-the-numbers/ (accessed June 10, 2015).

[4] R.W. Baker, Membrane Technology and Applications, 2nd ed. John Wiley & Sons, Ltd, Chichester, UK, 2004, http://dx.doi.org/10.1002/9781118359686.

[5] International Desalination Association, Desalination – An Overview, 2014 http://idadesal.org/desalination-101/desalination-overview/ (accessed June 10, 2015).

[6] A.S. Nafey, M.A. Sharaf, L. García-Rodríguez, Thermo-economic analysis of a combined solar organic rankine cycle-reverse osmosis desalination process with different energy recovery configurations, Desalination 261 (2010) 138–147, http://dx.doi.org/10.1016/j.desal.2010.05.017.

[7] G.P. Narayan, R.K. McGovern, S.M. Zubair, J.H. Lienhard, High-temperature-steam-driven, varied-pressure, humidification-dehumidification system coupled with reverse osmosis for energy-efficient seawater desalination, Energy 37 (2012) 482–493, http://dx.doi.org/10.1016/j.energy.2011.11.007.

[8] H. Cherif, J. Belhadj, Large-scale time evaluation for energy estimation of stand-alone hybrid photovoltaic–wind system feeding a reverse osmosis desalination unit, Energy 36 (2011) 6058–6067, http://dx.doi.org/10.1016/j.energy.2011.08.010.

[9] E.S. Hrayshat, Brackish water desalination by a stand alone reverse osmosis desalination unit powered by photovoltaic solar energy, Renew. Energy 33 (2008) 1784–1790, http://dx.doi.org/10.1016/j.renene.2007.11.001.

[10] A.M. Delgado-Torres, L. García-Rodríguez, Design recommendations for solar organic rankine cycle (ORC)–powered reverse osmosis (RO) desalination, Renew. Sust. Energ. Rev. 16 (2012) 44–53, http://dx.doi.org/10.1016/j.rser.2011.07.135.

[11] M. Ibarra, A. Rovira, D.C. Alarcón-Padilla, G. Zaragoza, J. Blanco, Performance of a 5 kWe solar-only organic rankine unit coupled to a reverse osmosis plant, Energy Procedia 49 (2014) 2251–2260, http://dx.doi.org/10.1016/j.egypro.2014.03.238.

[12] G. Xia, Q. Sun, X. Cao, J. Wang, Y. Yu, L. Wang, Thermodynamic analysis and optimization of a solar-powered transcritical CO2 (carbon dioxide) power cycle for reverse osmosis desalination based on the recovery of cryogenic energy of LNG (liquefied natural gas), Energy 66 (2014) 643–653, http://dx.doi.org/10.1016/j.energy.2013.12.029.

[13] L.-F. Liu, Z.-B. Cai, J.-N. Shen, L.-X. Wu, E.M.V. Hoek, C.-J. Gao, Fabrication and characterization of a novel poly(amide-urethane@imide) TFC reverse osmosis membrane with chlorine-tolerant property, J. Membr. Sci. 469 (2014) 397–409, http://dx.doi.org/10.1016/j.memsci.2014.06.029.

[14] M. Safarpour, A. Khataee, V. Vatanpour, Thin film nanocomposite reverse osmosis membrane modified by reduced graphene oxide/TiO_2 with improved desalination performance, J. Membr. Sci. 489 (2015) 43–54, http://dx.doi.org/10.1016/j.memsci.2015.04.010.

[15] J. Duan, Y. Pan, F. Pacheco, E. Litwiller, Z. Lai, I. Pinnau, High-performance polyamide thin-film-nanocomposite reverse osmosis membranes containing hydrophobic zeolitic imidazolate framework-8, J. Membr. Sci. 476 (2015) 303–310, http://dx.doi.org/10.1016/j.memsci.2014.11.038.

[16] M.H. Sharqawy, S.M. Zubair, J.H. Lienhard, Second law analysis of reverse osmosis desalination plants: an alternative design using pressure retarded osmosis, Energy 36 (2011) 6617–6626, http://dx.doi.org/10.1016/j.energy.2011.08.056.

[17] C. Knutson, Discussion of "second law analysis of reverse osmosis desalination plants: an alternative design using pressure retarded osmosis" [energy (2011) 36: 6617–6626], Energy 46 (2012) 688–690, http://dx.doi.org/10.1016/j.energy.2012.07.057.

[18] M.H. Sharqawy, S.M. Zubair, J.H. Lienhard, Rebuttal to "Discussion of 'Second law analysis of reverse osmosis desalination plants: an alternative design using pressure retarded osmosis' [Energy 2011] 36: 6617–6626],", Energy 46 (2012) 691–693, http://dx.doi.org/10.1016/j.energy.2012.08.035.

[19] L.D. Banchik, Osmotic Mass Exchangers for Power Generation and Energy Recovery : Analysis and Analogy to Heat Exchangers, Massachusetts Institute of Technology, 2013.

[20] R.L. Truby, Seawater desalination by ultralow-energy reverse osmosis, in: N.N. Li, A.G. Fane, W.S.W. Ho, T. Matsuura (Eds.), Adv. Membr. Technol. Appl. John Wiley & Sons, Inc., 2008

[21] L. Fitzsimons, B. Corcoran, P. Young, G. Foley, Exergy analysis of water purification and desalination: a study of exergy model approaches, Desalination 359 (2015) 212–224, http://dx.doi.org/10.1016/j.desal.2014.12.033.

[22] M.H. Sharqawy, J.H. Lienhard V, S.M. Zubair, On exergy calculations of seawater with applications in desalination systems, Int. J. Therm. Sci. 50 (2011) 187–196, http://dx.doi.org/10.1016/j.ijthermalsci.2010.09.013.

[23] Y. Cerci, Improving the Thermodynamic and Economic Efficiencies of Desalination Plants, University of Nevada, 1999.

[24] Y. Cerci, Exergy analysis of a reverse osmosis desalination plant in California, Desalination 142 (2002) 257–266, http://dx.doi.org/10.1016/S0011-9164(02)00207-2.

[25] A. Bejan, G. Tsatsaronis, M. Moran, Thermal Design and Optimization, John Wiley & Sons, Inc., New York, 1996.

[26] A. Bejan, Advanced Engineering Thermodynamics, 3rd ed. John Wiley & Sons, Inc., New Jersey, 2006.

[27] N. Kahraman, Y.A. Cengel, B. Wood, Y. Cerci, Exergy analysis of a combined RO, NF and EDR desalination plant, Desalination 171 (2004) 217–232, http://dx.doi.org/10.1016/j.

[28] Y. Demirel, Thermodynamic analysis of separation systems, Sep. Sci. Technol. 39 (2004) 3897–3942, http://dx.doi.org/10.1081/SS-200041152.

[29] K.H. Mistry, R.K. McGovern, G.P. Thiel, E.K. Summers, S.M. Zubair, J.H. Lienhard V, Entropy generation analysis of desalination technologies, Entropy 13 (2011) 1829–1864, http://dx.doi.org/10.3390/e13101829.

[30] T.J. Kotas, The Exergy Method of Thermal Plant Analysis, Butter-Worths, London, UK, 1985.

[31] R.L. Cornelissen, Thermodynamics and Sustainable Development: The use of Exergy Analysis and the Reduction of Irreversibility, University of Twente, The Netherlands, 1997.

[32] L. Fitzsimons, A Detailed Study of Desalination Exergy Models and Their Application to a Semiconductor Ultra-Pure Water Plant, Dublin City University, 2011.

[33] I.H. Aljundi, Second-law analysis of a reverse osmosis plant in Jordan, Desalination 239 (2009) 207–215, http://dx.doi.org/10.1016/j.desal.2008.03.019.

[34] A. Gasmi, J. Belgaieb, N. Hajji, Technico-economic study of an industrial reverse osmosis desalination unit, Desalination 261 (2010) 175–180, http://dx.doi.org/10.1016/j.desal.2010.04.060.

[35] A.M. Blanco-Marigorta, M. Masi, G. Manfrida, Exergo-environmental analysis of a reverse osmosis desalination plant in Gran Canaria, Energy 76 (2014) 223–232, http://dx.doi.org/10.1016/j.energy.2014.06.048.

[36] J. Liu, J. Yuan, L. Xie, Z. Ji, Exergy analysis of dual-stage nanofiltration seawater desalination, Energy 62 (2013) 248–254, http://dx.doi.org/10.1016/j.energy.2013.07.071.

[37] V. Romero-Ternero, L. Garcia-Rodriguez, C. Gomez-Camacho, Exergy analysis of a seawater reverse osmosis plant, Desalination 175 (2005) 197–207.

[38] F. Macedonio, E. Drioli, An exergetic analysis of a membrane desalination system, Desalination 261 (2010) 293–299, http://dx.doi.org/10.1016/j.desal.2010.06.070.

[39] M.H. Sharqawy, J.H. Lienhard, S.M. Zubair, Thermophysical properties of seawater: a review of existing correlations and data, Desalin. Water Treat. 16 (2010) 354–380, http://dx.doi.org/10.5004/dwt.2010.1079.

[40] S.R. Turns, Thermodynamics: Concepts and Applications, Cambridge University Press, New York, 2006.

[41] C. Fritzmann, J. Löwenberg, T. Wintgens, T. Melin, State-of-the-art of reverse osmosis desalination, Desalination 216 (2007) 1–76, http://dx.doi.org/10.1016/j.desal.2006.12.009.

[42] Energy Recovery Inc. ERI Power Model., http://www.energyrecovery.com/resource/power-model/ (accessed April 09, 2015).

[43] M.H. Sharqawy, L.D. Banchik, J.H. Lienhard, Effectiveness–mass transfer units (ε–MTU) model of an ideal pressure retarded osmosis membrane mass exchanger, J. Membr. Sci. 445 (2013) 211–219, http://dx.doi.org/10.1016/j.memsci.2013.06.027.

[44] S.A. Klein, Engineering Equation Solver. Academic Professional Version 9.698, http://www.fchart.com/ees/ees.shtml.

[45] A. Achilli, A.E. Childress, Pressure retarded osmosis: the vision of Sidney Loeb to the first prototype installation — review, Desalination 261 (2010) 205–211, http://dx.doi.org/10.1016/j.desal.2010.06.017.

[46] F. Helfer, C. Lemckert, Y.G. Anissimov, Osmotic power with pressure retarded osmosis: theory, performance and trends — a review, J. Membr. Sci. 453 (2014) 337–358, http://dx.doi.org/10.1016/j.memsci.2013.10.053.

[47] L.D. Banchik, M.H. Sharqawy, J.H. Lienhard, Limits of power production due to finite membrane area in pressure retarded osmosis, J. Membr. Sci. 468 (2014) 81–89, http://dx.doi.org/10.1016/j.memsci.2014.05.021.

[48] A. Achilli, T.Y. Cath, A.E. Childress, Power generation with pressure retarded osmosis: an experimental and theoretical investigation, J. Membr. Sci. 343 (2009) 42–52, http://dx.doi.org/10.1016/j.memsci.2009.07.006.